ENGINEER - Vol. LV, No. 04, pp. [47-60], 2022

DOI: http://doi.org/10.4038/engineer.v55i4.7543

Development and Performance Analysis of a Small-Scale On-shore Wave Energy Converter

B.J.C.L. Jayathunga and H.C.P. Karunasena

Abstract: Many renewable energy sources are being exploited at a higher rate due to the increasing demand for cleaner and cheaper energy. However, sea wave energy extraction remains one of the least-developed renewable energy sources despite its high energy density and availability compared to many other renewable energy sources. Accordingly, this work aimed to develop a small-scale sea wave energy converter (WEC) to be deployed in a non-shore configuration for power generation. A device was designed to extract both the kinetic and potential energies from sea waves aiming for higher overall energy extraction efficiency. It is composed of a set of flaps and a floater, which are rigidly connected to a frame allowing them to interact with incoming waves. Following the concept, a small-scale model with 35 W capacity was fabricated and tested in a coastal location near Galle, Sri Lanka, having waves of approximately 1 m wave height and a 20 s wave period. It was observed that the device could extract power continuously, yielding an average power output of 1.45 W and an overall efficiency of 4.143%. Wave irregularities, sand particle interaction, and frictional losses in mechanism were observed to be hindering the performance of the convertor, which need to be addressed in the future.

Keywords: Ocean energy, On-shore wave energy converter, Renewable energy, Small-scale wave energy convertor, Wave energy conversion

1. Introduction

Even though the interest in the application and development of renewable energy technologies remains high, most of the world's energy needs are still being fulfilled by non-renewable energy sources. Some of the key problems associated with non-renewable energy sources are the high costs and declining fuel reserves given the current consumption patterns, adverse environmental impacts which are becoming of utmost importance in the present context in both climate change, and public health concerns [1]. While wind energy and solar energy are the key renewable energy resources that have been harnessed to greater extents, wave energy can also be considered as a promising renewable energy source where the estimated global coastal wave power extraction potential is about 2 terra watts[2]. However, due to many technical and economic challenges, still the wave energy extraction cannot be identified as a commercially available power generation method [3]. In this background, when Sri Lanka is considered, wave energy extraction should be given greater priority since there is a definite potential of generating sufficient renewable power since the island nation has a long coastline of about 1400 km with a sufficient number of candidate sites for wave power generation with higher wave power potential in the range of 10-15 kW per 1 m length of the wave crest [4, 5].

In the international context, the first patent of a Wave Energy Convertor (WEC) had been filed in 1799, and thereafter, many WEC technologies have been developed based on different operational principles. These devices can be categorised into three types based on their installation location: (a) on-shore or coastline devices; (b) near-shore devices which are installed at moderate water depths (<20 m depth); and (c) offshore devices (>20 m depth) [6]. Commonly used types of wave energy converters are either overtopping type, oscillating water column type, or oscillating body type, which can be fully submerged or partially submerged in the sea.

*Eng. **B.J.C.L. Jayathunga**, AMIE(SL), AEng, AMSLEMA, BSc. Eng. (Hons.) (Ruhuna)*
Email:charaka.jayathunga@gmail.com
http://orcid.org/0000-0002-0556-8282
*Eng. (Prof.) **H.C.P. Karunasena**, AMIE(SL), AEng, PhD (QUT), MSc (Moratuwa), BSc. Eng. (Hons.) (Moratuwa), Professor, Department of Mechanical and Manufacturing Engineering, Faculty of Engineering, University of Ruhuna, Hapugala, Galle, Sri Lanka*.*
Email:chaminda@mme.ruh.ac.lk
https://orcid.org/0000-0002-4203-831X

* Author affiliation institution was corrected.

The majority of the WEC technology development in Europe is focused on the point absorber type, where an oscillating body is used to capture the wave energy. These systems can be used as independent generators or as part of offshore infrastructure such as breakwaters. Most of these systems are still in the development stage and rated capacities are in the range of 15 to 6000 kW. Furthermore, other overtopping and oscillating water column device technologies are also in the operational or development stages [7]. An overtopping device mainly captures the potential energy of sea waves, where the incident wave is captured in an inbuilt elevated reservoir such that the captured seawater is passed through hydro turbines, generating power.

Oscillating water column (OWC) devices are typically built on or near the shore. These devices utilise the oscillating nature of the seawater to drive an air turbine. An OWC device contains a chamber which is open to the sea from the bottom. The upper part of the chamber is exposed to the atmosphere through a duct which houses an air turbine. When an incident wave approaches the device, the water level inside the chamber rises, thus pushing the air inside the chamber to the atmosphere through the duct. Generated air flow drives the air turbine, giving out mechanical power. When the water level drops below the mean sea level, air is sucked into the chamber, providing power to the air turbine. Here, Wells turbines are frequently used, designed specially to rotate in a single direction regardless of the airflow direction, making the power take-off more effective [8].In terms of performance of WECs, oscillating body type devices, oscillating water column devices and overtopping devices have efficiencies in the range of 16-79%, 20-30% and 12-27%, respectively [9].

In terms of wave energy conversion technologies, the main cost components are initial investment (34%), operation and maintenance cost (40%), replacement (25%), and pre-operating costs and decommissioning costs (1%) [10]. When operation and maintenance (O&M) costs and replacement costs are combined, it represents 65% of the total project cost. Since O & M costs and replacement costs contribute to the most significant cost component of a wave energy project (i.e.almost 2/3), it is of great importance to develop technologies that have reduced O&M costs and replacement costs for a project to be economically viable. O&M cost can be excessively high when accessibility to the device is limited, especially to the power conversion system which often requires regular maintenance. Hence, considerable cost reductions are possible when WEC systems are at easily accessible locations (ideally on land), leading to lower costs.

Since both potential and kinetic energy types are included in the total wave energy in equal proportions, a wave energy conversion device can become more efficient resulting in low cost of energy, making wave energy projects more economically viable. However, majority of the devices that have been developed so far have mainly focused on capturing only one type of energy and hence, 50% of the energy is left out by design.

On this basis, this paper presents a development of an on-shore based tethered wave energy converter, which can extract both kinetic and potential energies of waves while the power conversion system is mounted on the seashore, with the aim of minimising the operation and maintenance costs. The paper is organised such that Section 2 includes a brief overview of the theoretical background of wave energy extraction technologies and state of the art. In Section 3, the methodology of the research is presented and in Section 4, simulation results and experimental results based on field tests of the model are presented. Finally, the key conclusions and future works are elaborated in Section 5.

2. Wave Energy Extraction

Sea waves are generated due to the frictional effects of the wind flowing over the free surface of the ocean. Compared to the wind, waves own a higher energy density, hence harvesting energy from waves can be considered as more effective than directly from air. However, strong winds and stormy conditions can sometimes create even more energetic yet destructive waves, which can cause damage to the WECs [11]. To design efficient and effective WECs, it is very important to understand the fundamentals involved with the sea waves. For instance, the energy contained in sea waves is transmitted in the direction of wave propagation, while water particles in the sea water primarily undergo oscillatory motions before wave breaking. After the wave break, most of the energy contained in the wave is lost to overcome the surface tension, viscous forces, and turbulent flow fields. Hence, the optimum locations to capture wave energy are located just before the wave break. The power potential contained in sea waves can be expressed as the wave power flux per unit length of a wave crest P_W, defined as follows [7].

$$P_W = \frac{\rho g^2}{64\pi} T_e H_s^2 \qquad \ldots(1)$$

where ρ is the density of seawater, g is the gravitational acceleration, T_e is the wave energy period and H_s is the significant wave height. This can be further simplified as follows.

$$P_W = 0.5 H_s^2 T_e \qquad \ldots(2)$$

Where, wave power flux P_W is in kW/m when the significant wave height H_s is in meters and the wave energy period T_e is in seconds. To capture this power, a wave energy converter can be designed and installed in a way that it interacts with incoming waves creating a destructive interference. This way, the energy contained in the wave is dissipated and absorbed by the wave energy converter. In order to maximise energy harvesting, wave energy converters may be installed to form an array in a given wave field. However, due to practical constraints, harnessing of all the energy in the waves by using a wave energy converter is not possible. In order to evaluate wave energy converters for their performance, the Capture Width Ratio (η) is used and is defined as follows[7].

$$\eta = \frac{P_E}{P_W} \qquad \ldots(3)$$

where, P_E is the power absorbed by the wave energy converter. Accordingly, the WEC designed in this work mainly focused to improve η and the following Section presents details of its design and construction.

3. Methodology

3.1 Design Overview

The design phase was initiated with the conceptualisation of different possible device configurations to optimise harnessing of the sea wave energy and a detailed functional block diagram was developed in this regard as shown in Figure 1. By thoroughly analysing wave mechanics, local sea states, and operational requirements of the WEC, six concepts were devised and the most promising one was deduced using a weighted-objective analysis, based on key design objectives such as power tapping capability, conversion efficiency, transmission efficiency, fabrication cost, scalability, fabrication simplicity, and maintenance cost.

The most promising concept involves two main components: a submerged power take-off system and a shore-mounted power conversion system. Coupling of these two systems was achieved by a cable-chain transmission mechanism. The working block diagram of the proposed design is given in Figure 2.The submerged power take-off system has a bottom-mounted rigid frame with the ability to mount it firmly to the seabed. Another structural member (lower strut) is there to connect the mentioned frame at one end using a universal joint which allows it to move in a 3-D working envelope. A third frame (upper strut) which has a buoy and a set of flaps rigidly connected to it, is attached to the lower strut in a manner that only allows 1 degree-of-freedom (DoF) in the upper strut, i.e., the upper strut is only allowed to move translationally relative to the lower strut. When this relative translational motion is combined with the motion of the lower strut, the total working envelope of the device covers an inverted conical 3-D space as given in Figure 3.

Apart from the submerged power take-off mechanism, the proposed device also comprises a shore-mounted power conversion system that converts the absorbed power into electricity. Transmission of power from the power take-off system to the conversion system is achieved by connecting the two systems using a cable-chain arrangement where two cables are attached at the power take-off side and two individual chains are attached to the other end of each cable, towards the power conversion system. The connection between the cable and the chain is accomplished by a special swivel hook which prevents twisting of the chain regardless of the twisting of the cable. Counterweights that provide restoration force to the power take-off components are attached to the free ends of the chains, and chains are arranged to pass over one-way sprockets mounted on a shaft. The shaft is coupled to an electric generator through a gearbox. Therefore, once the power take-off system interacts with the incoming sea waves, the motion of the power take-off components causes the cable-chain arrangement to become stretched which in turn rotates the shaft mounted on the power conversion system, initiating electricity generation.

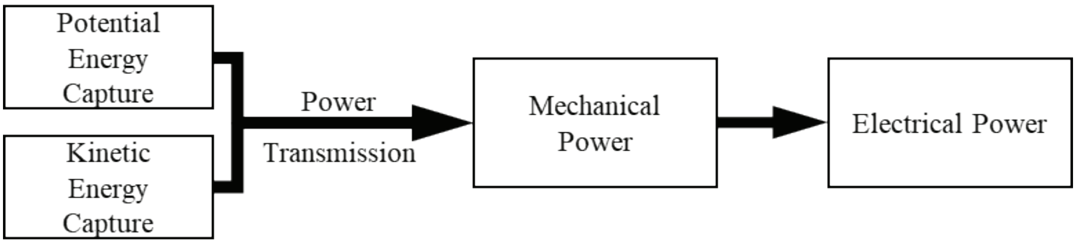

Figure 1 - Functional Block Diagram of the Proposed WEC

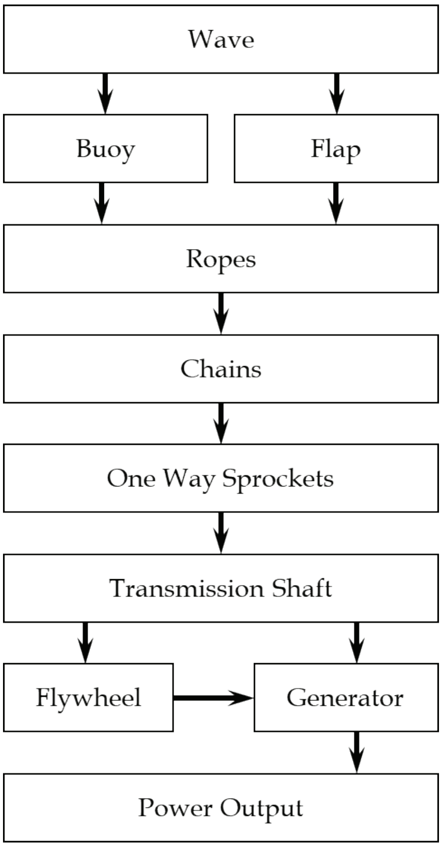

Figure 2 – Functional Block Diagram of the Proposed WEC

As a result of the restoration force applied by the counterweights on the power take-off system, it immediately regains its initial position once the upward excitation of a given wave is no longer available. A 3-D model of this WEC developed by SolidWorks (version 2016) is shown in Figure 4.

3.2 Forces Acting on the Device

3.2.1 Froude-Krylov Force

Froude-Krylov force is the force acting on a body due to the pressure exerted on the wetted surface of that body. Froud-Krylov force can be calculated by integrating the pressure field over the wetted surface of the body. Both the static and dynamic components of the Froude-Krylov force are given by the following Equations [12].

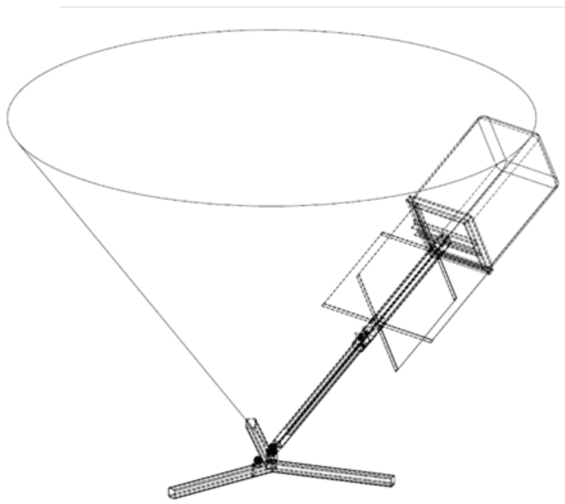

Figure 3 - Working Envelope of the Submerged Power Take-Off System of the Proposed WEC

$$F_{FK,st} = F_g + \iint_{S(t)} -\gamma z n dS \qquad \ldots(4)$$

$$F_{FK,dy} = \iint_{S(t)} p_{dy} n dS \qquad \ldots(5)$$

where, $n = (n_x, n_y, n_z)$ is the unit vector normal to the surface, pointing outwards, F_g is the gravity force, $-\gamma z$ is the static pressure defined according to the inertial reference frame (x, y, z) with the origin at the still water level, x aligned with the direction of wave propagation, z pointing upwards and p_{dy} represents the dynamic pressure.

3.2.2 Diffraction Force

Together with the Froude-Krylov force, diffraction force makes up the total non-viscid hydrodynamic force acting on the WEC body. Diffraction force can be computed using the linear potential theory using the following equation[13].

$$F_D = \int_0^t K_D(t-\tau)\eta(\tau)d\tau \qquad \ldots(6)$$

where, $K_D(t)$ is the diffracted force associated with an impulsive free surface elevation propagating along the x-axis and $\eta(\tau)$ is the free surface elevation at a given reference location.

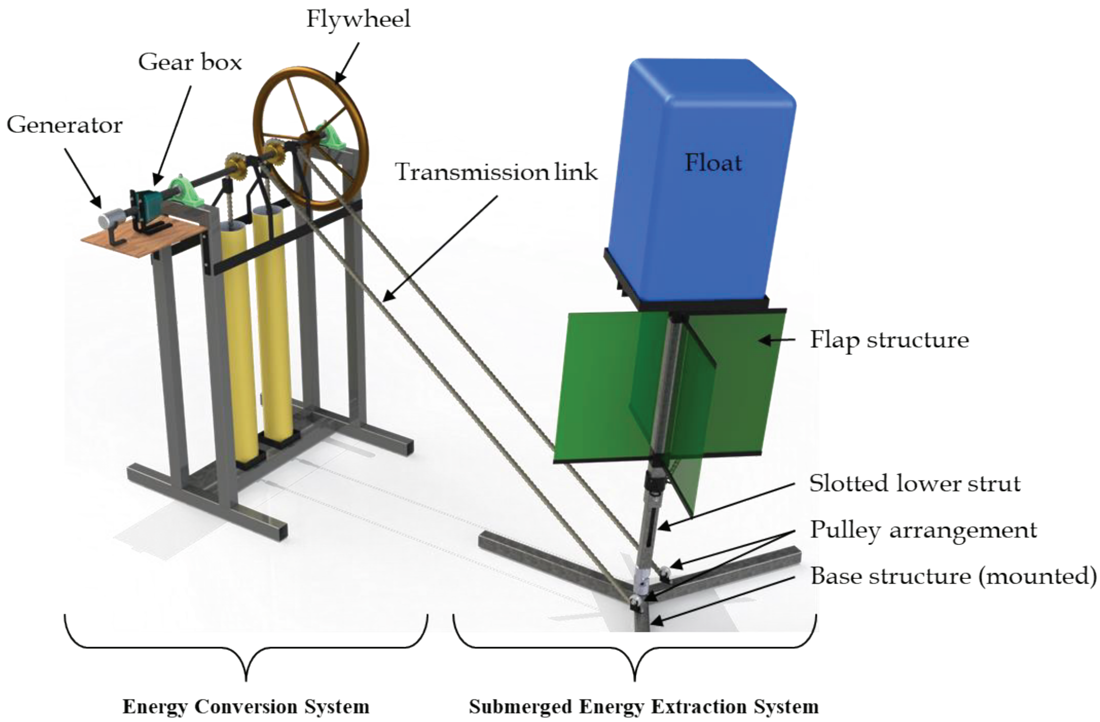

Figure 4 – 3-D Model of the Proposed WEC

3.3 Parameters of the Design

The physical and geometrical parameters of the proposed WEC are given in Table 1. Dimensions of the main components which are associated with power take-off play an important role in the overall device performance, hence dimensions should be chosen carefully based on the topography of the seabed and considering available sea state at the location where the device is to be deployed. In this design, the potential test site was investigated preliminarily to select the dimensions of the device. Since both the kinetic energy and potential energy of the sea waves are to be harnessed by the WEC, buoy and flap dimensions are to be chosen to match the expected total power output.

Table 1 - Initial Parameters of the Device

Parameter	Size of the Component	
	Buoy	Flap
Shape	Cuboidal	Prismatic Shell
Height (m)	0.400	0.500
Width (m)	0.300	0.425
Projected area perpendicular to flow direction (m^2)	0.1200	0.2125
Volume (m^3)	0.036	-
Weight (Approx.) (kg)	5.0	8.0

In this WEC, the buoy acts as an oscillating body that moves translationally relative to the frame to which it is attached once the buoy interacts with the incoming sea waves. Combined with the DOF of the frame to which the buoy is attached, the buoy is capable of performing circular orbital movement which is ideal for efficient power absorption since bodies that move in circular orbits are more effective in wave power absorption [14].

Weight and the volume are critical factors which decide the dynamics of the upward motion of the buoy, where higher the volume and lower the weight, the quicker the buoy response. However, for the downward motions, these two factors influence in the opposite way. This is the other way around for the downward motion of the buoy. To be effective in the power take-off, the response time of the buoy should match the wave period. Hence, the selected buoy should have weight and volume values that satisfy the above-mentioned criterion.

Since, in the proposed device, flaps contribute to harvest a significant portion of energy contained in the sea waves through surge motion, determination of an optimum flap profile is crucial, considering operational characteristics as well as ease of fabrication and to minimise the cost involved. To determine the optimum flap profile, CFD simulations were carried out in the 2-D domain on two selected geometrical profiles to evaluate their relative performance to be used as flaps. ANSYS Fluent 19.0 was used for the said numerical simulations which were performed on a computer with Intel Core i5 4210H processor having a RAM of 8 GB. In these simulations, the drag coefficient of the flap system was used to identify the best profile where the flap system with profiles that characterise the highest drag coefficient was identified as optimal. Parameters of the analysed flap profiles are given in Table 2. Furthermore, Figure 5 represents the 2-D geometrical shapes of the respective flap profiles.

Table 2 - Geometrical Parameters of the Analysed Flap Profiles

Flap Type	Prismatic Shell	Semi-cylindrical Shell
Number of flaps	4	3
Flap Arrangement	90˚ apart	120˚ apart
Projected Dimensions (m) (Width × Height)	0.425 × 0.500	0.450 × 0.500
Total Projected Area (m^2)	0.2125	0.2250

Furthermore, CFD analyses were performed on the proposed device using ANSYS Fluent 19.0 to predict the forces acting on the device components. In these finite element analyses (FEA), the load acting on the transmission system of the device was predicted for different device orientations in sea waves and were used to optimise the device for both operational performance and reliability under extreme forces. Accordingly, key design specifications of the proposed device were derived and are presented in Table 3.

3.4 Experimental Phase

Measurement setup for the experimental phase was composed of a constant-friction load applied on the output shaft of the WEC, an arrangement to count the number of revolutions made by the output shaft under the applied load, and a stopwatch to keep a record of time. A schematic diagram of the mechanical components of the measurement system is given in Figure 6 and its parameters are given in Table 4.

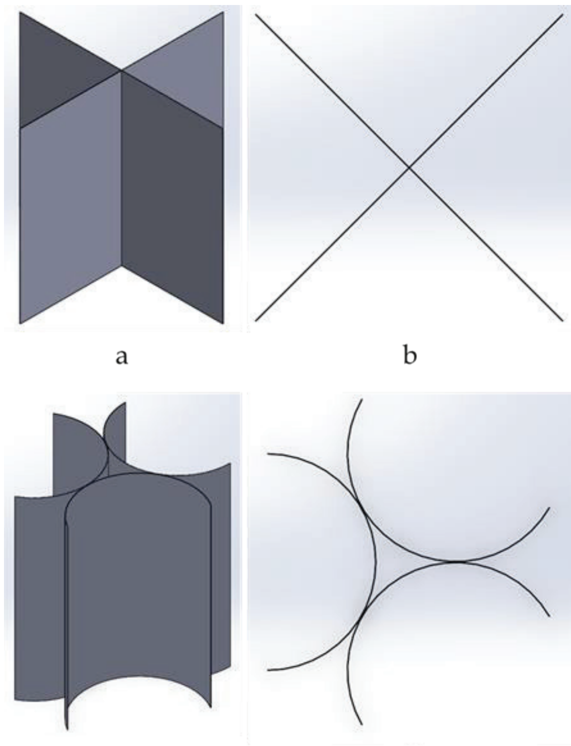

Figure 5 – (a) Prismatic Shell Flap Arrangement Isometric View and (b) Top View, (c) Semi-Cylindrical Shell Flap Arrangement Isometric View and (d) Top View

Table 3 – Device Specifications

Motion	All Directional
Power Tapping Modes	Heave and Surge
Transmission	Cables and Chain
Flap Shape	Prismatic Shell
Buoy Shape	Cuboidal
Buoy Volume (m^3)	0.036
Maximum Heaving Stroke (m)	0.5

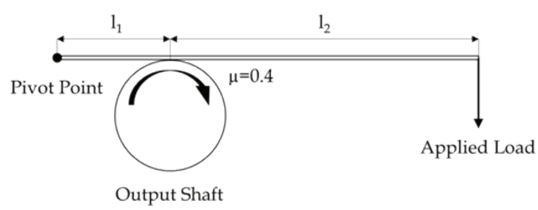

Figure 6–Schematic of Energy Measurement system

The total energy produced by the device (E_{output}) can be derived as given in Eq. 7, with the use of the total shaft rotation angle and the applied load. Here, μ, m, g, l_1, l_2 and D are friction coefficient, applied load, gravitational acceleration, distance from pivot point to the contact point, distance from applied load to the contact point, and the output shaft diameter, respectively.

$$E_{output} = \frac{\mu m g l_2 D \theta}{2 l_1} \qquad \ldots(7)$$

For a given time t, the average power output can be computed by Eq. 8 where, $P_{output\ avg}$ is the average power output for the time period considered.

$$P_{output\ avg} = \frac{E_{output}}{t} \qquad \ldots(8)$$

Table 4 - Measurement System Parameters

Parameter	Value
Shaft Diameter - D(m)	0.02
Applied Load - m(kg)	0.80
Friction Coefficient - μ	0.40
Distance from pivot to contact point - l_1(m)	0.06
Distance from applied load to contact point - l_2(m)	0.19

4. Results and Discussion

4.1 Simulation Results of the Flaps

Flow simulation results for the two-flap arrangements are given in Figure 7 and Figure 8. The CFD model was validated for the drag coefficient against already published data and an agreement within 5% of error was obtained for both the geometrical shapes [15]. Based on the results for the induced drag on each flap arrangement, it is evident that the prismatic shell-type flap arrangement having a drag coefficient of 1.97 is more effective in capturing the incoming kinetic portion of the wave energy than the semi-cylindrical flap arrangement which only has a drag coefficient of 1.08. When subjected to a uniform sea water flow at a velocity of 2 m/s, the total drag force induced on the cylindrical shell type flap arrangement was found to be only 498.15 N, compared to the 853.82 N induced on the prismatic shell type flap. Since the force imparted on the flap arrangement directly contributes towards the extraction of kinetic energy from sea waves, flap arrangement should have a high tendency to disrupt the fluid flow, thus being subjected to a drag force. Based on the results of the CFD analyses, it is evident that the main contributor of the total drag force is the shape according to Figure 8. When comparing the pressure contours for the prismatic shell type flap and semi-cylindrical shell type flap in Figure 8, the prismatic shell type flap arrangement shows a larger pressure variation in the upstream and downstream of the flow. The low-pressure region created by the prismatic shell type flap arrangement is relatively larger compared to the semi-cylindrical flap arrangement. Furthermore, when comparing the maximum pressure on the two flap types, prismatic shell type flap is subjected to the highest pressure. Therefore, the pressure drag on the prismatic shell type flap can be taken as higher than that of the semi-cylindrical type flap. Tendency for being subjected to high drag forces also improves the responsiveness of the power take-off system, making the device more effective in energy extraction.

When looking at the pressure contours of the cylindrical shell type flap arrangement, several low-pressure regions between two adjacent flaps can be identified. This low pressure imparts additional forces on the flaps increasing the stress the flaps are subjected to. Such stresses can lead to premature failure since theses loads can be seen as cyclic throughout the operation of the device as the loading is due to wave interaction with the device. However, such a problem cannot be identified for prismatic shell type flaps. Thus, with respective to the strength also, prismatic shell type flaps can be more beneficial.

4.2 Hydrodynamic Simulation Results

To determine the forces exerted on the power take-off system of the device, hydrodynamic simulations were conducted using ANSYS AQWA 19.0. The 3-D model of the power take-off system of the device was converted to a compatible geometry and was used for the analysis. Simulation results were used to size the device components.

Details of the simulation model are given in Table 5, while Figure 9 shows the model used for the simulation. To simplify the simulation model, a hinged joint with 1 DoF was modeled connecting the power take-off mechanism and the sea floor. Forces exerted by the waves on the device are directly transferred to this joint. As per the design of the proposed device, force exerted on the power take-off mechanism is transferred in the form of a rope tension up to the power conversion system. Hence the force on the joint directly correlates to the power take-off potential of the device. Therefore, hydrodynamic simulations were used to calculate the force on the joint to evaluate the power take-off potential of the system. Time varying joint forces are given in Figure 10 and Figure 11.

When looking at individual force components, X-direction force shows a significant variation compared to Z-direction force. Constant interaction with passing water in the X-direction can be the reason for this while the Z-direction force largely depends upon the passing of the wave which only occurs periodically. X-direction force peaks at around 170 N when compared to 290 N magnitude of Z-direction force. Even though the magnitude of the X-direction force is significantly less than that of the Z-direction force, it is evident that the horizontal component of the joint force (X-direction force) also can be utilised to extract energy when a suitable power take-off arrangement is employed. Thus, both the surge effect (X-direction movement) and the heave effect (Z-direction movement) of the device can be used to extract energy from sea waves making the device capable in extracting both the kinetic and potential energy.

Figure 11 shows the total joint force over time. Here, the total joint force has been calculated by considering the magnitudes of x-direction and z-direction forces acting on the device. This joint force is the main driving force of the power conversion system. Based on the simulation results, the maximum joint force was found to be 349.0 N which occurs at each wave interaction at a time gap of 15 s. Immediately following the peak joint force at each wave pass, relatively smaller magnitude forces are also exerted in the form of oscillations between consecutive occurrence speaking at 100 N. This can be due to the slamming force generated when the device hits the free water surface below its highest point of actuation. This can be avoided by optimising the inertia properties of the device to match its frequency domain response with the waves. Total joint force should be considered when sizing components of the device to make them withstand the wave load. Special attention should be given to the joint, flap structure and the base structure as these locations are mostly prone to damage when subjected to wave loading.

4.3 Experimental Results

In this research, all the experiments were carried out in a coastal area located in Gintota, Galle, Sri Lanka (GPS location: 6.051073, 80.181529) and two sets of experiments were performed. Figure 12 shows the fabricated device in operation in the sea at the selected location. Energy extraction system was submerged in the sea and connected to the power conversion system using two tethers which consist of a combination of a Nylon rope attached to the energy extraction system and a chain coupled to the power conversion system. In each of the experiments, the average mechanical energy output from the device was measured at different instances throughout the duration of each of the experiments. Obtained data was used to calculate the average power during the trials. A summary of experimental results obtained during the field tests are given in Table 6.

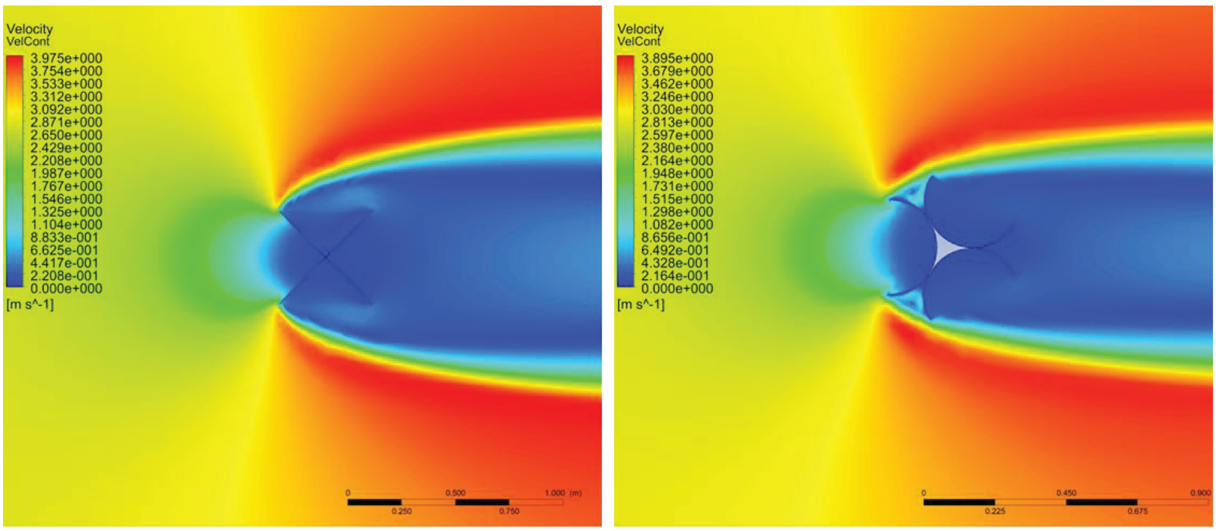

a b

Figure 7 - Velocity Contours for, (a) Prismatic Shell Flap Arrangement and (b) Semi-Cylindrical Shell Flap Arrangement

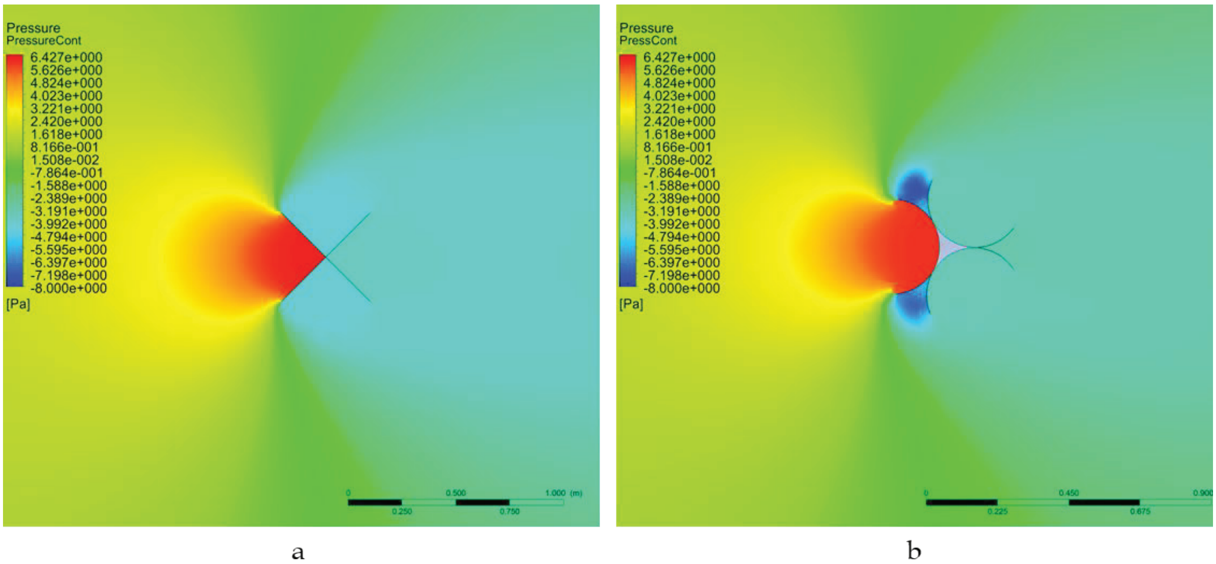

Figure 8 - Pressure Contours for, (a) Prismatic Shell Flap Arrangement and (b) Semi-Cylindrical Shell Flap Arrangement

Table 5 – Parameters used for the CFD Simulations

Mass information	13 kg (I_{xx}=1.88 kg m^2, I_{yy}=1.88 kg m^2, I_{zz}=0.21 kg m^2
Joint information	Hinged joint rotatable about Y axis
Mesh information	Total elements=4589 Diffracting elements=3588
Analysed wave frequencies	0.016 Hz to 1.000 Hz
Analysed wave directions	8 equally spaced directions from -180^o to 180^o
Computation type	Time response analysis followed by diffraction analysis
Analysis type	Regular wave response
Wave parameters	Wave height = 0.6 m Wave period = 15.0 s Wave frequency = 0.0667 Hz
Time step	0.05 s
Total simulation time	50.0 s
Processor information	Intel Core i5-4210H processor
Memory	8 GB
Simulation clock time	47 minutes (2820 seconds)

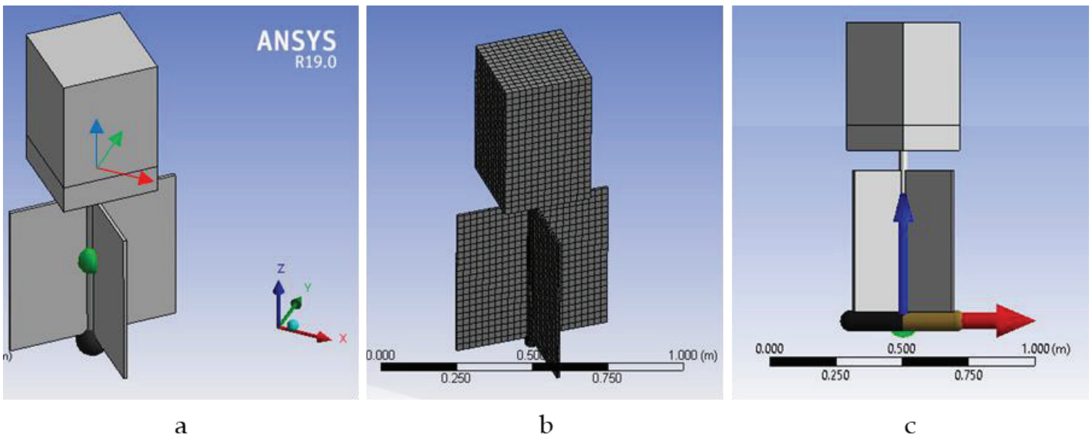

Figure 9–Ansys Simulation Model: (a) Geometry, (b) Mesh, and (c) Geometry with the Modeled Hinged Joint

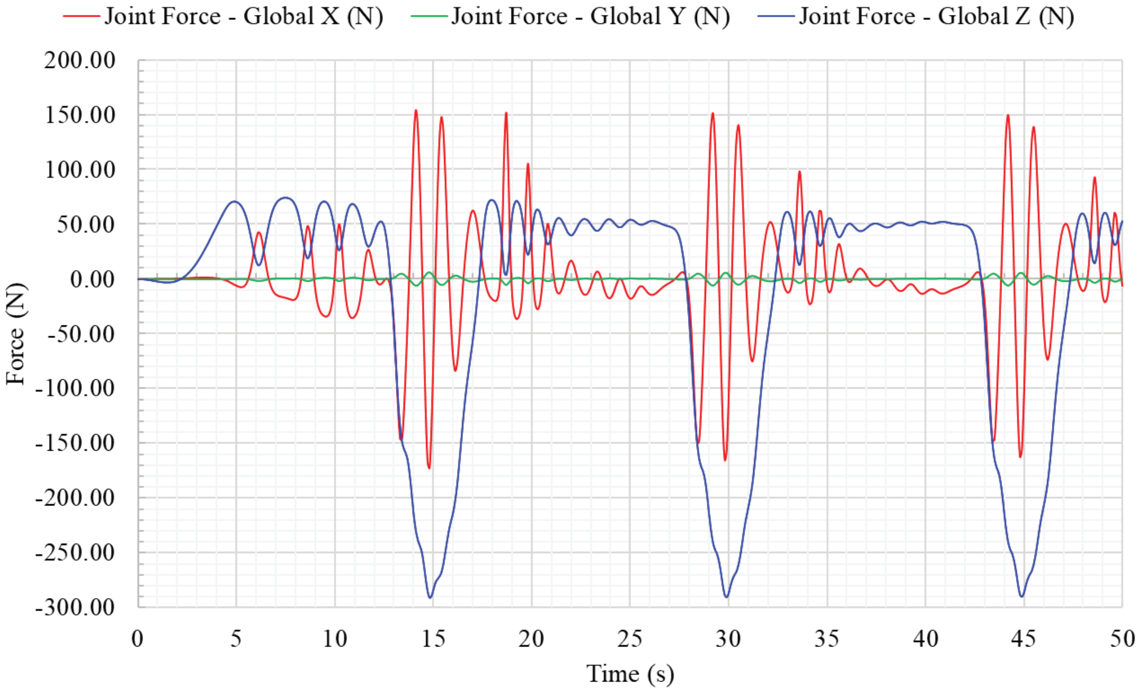

Figure 10 – Simulation of Forces on the Hinged Joint

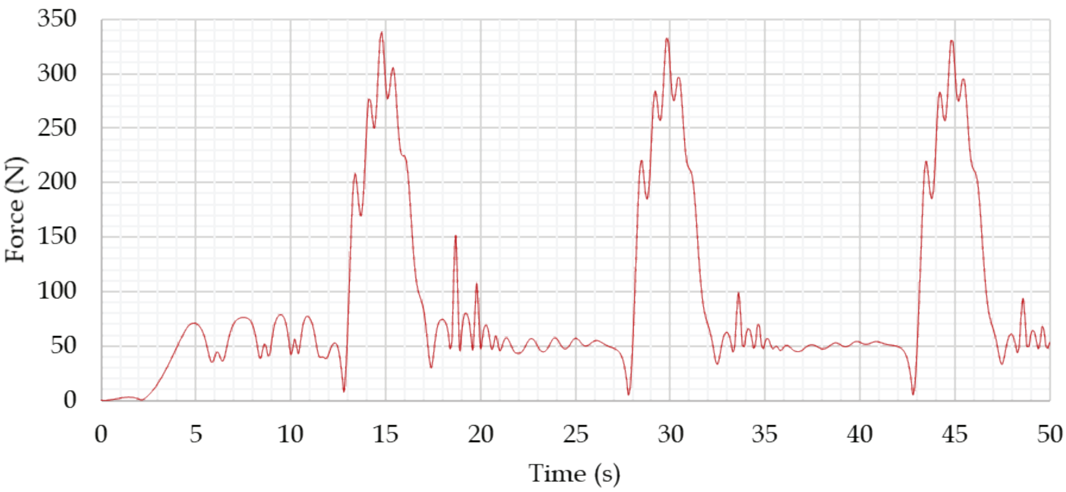

Figure 11 – Variation of the Magnitude of the Total Joint Force Over Time

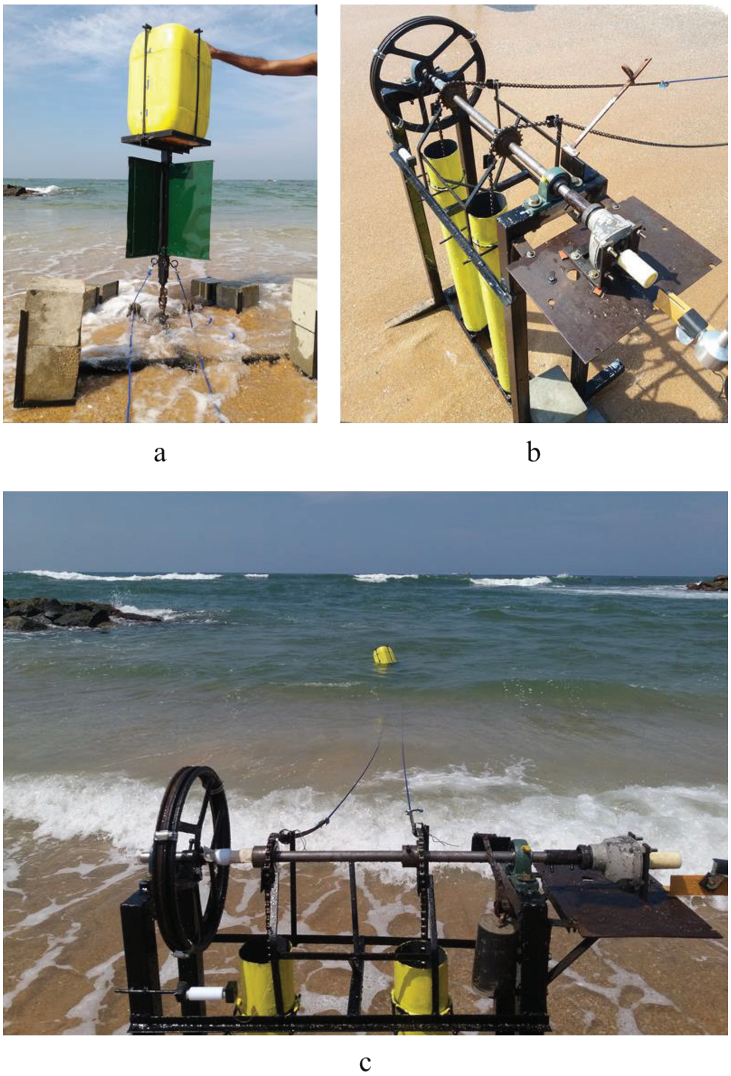

Figure 12 - Fabricated WEC Installed in the Experimentation Cite: (a) Energy Extraction System before Deployment, (b) Energy Conversion System before Deployment, and (c) Device in Operation

Table 6 - Experimental Results

	1st Deployment			2nd Deployment		
Instance	**1**	**2**	**3**	**1**	**2**	**3**
Total Extracted Energy (J)	30.3	18.1	15.7	464.8	432.5	465.6
Observed Time (s)	215	127	113	320	300	320
Power (W)	0.141	0.142	0.139	1.453	1.442	1.455
Average Power Output (W)	0.141			1.450		

During the first deployment, the device only showed a very limited performance amounting only to 0.141 W average power output. When the device behaviour was observed during the deployed duration, it was noted that the mounted base structure was not rigid enough to keep the submerged energy extraction system in place. This resulted in undesired movements of the whole energy extraction system, leading to lower performance. To overcome this drawback, for the second deployment, the base structure was modified to be more rigid by increasing the anchoring weight and adding spikes to the bottom to benefit from the skin friction. Furthermore, observations during the first deployment revealed that the device response to incoming waves was very slow, mainly due to mismatch between the device dimensions and topography of the seabed and the incoming wave characteristics. Accordingly, the dimensions of the device and other parameters such as assembly weight were adjusted in the second deployment to make the device more responsive to custom wave conditions at the selected location. This modification allowed the device to perform synchronously with the incident waves. Another main problem identified during the first deployment was chains coming off the sprockets. To correct this, chain guides were added to keep the chains in place.

Following the mentioned modifications, it was revealed that the device arrangement made it ideal for ease of installation without requiring complex arrangements. Also, placement of the power conversion system on-shore, out of the seawater proved to be beneficial in reducing operation and maintenance efforts by making accessibility and repairing more convenient than in cases of offshore or submerged power conversion systems. However, maintenance of the submerged power extraction system remains a challenge when the device is deployed, thus certain modifications may be required to make underwater maintenance works convenient.

When comparing the efficiency values observed at the two deployments (with respect to designed power extraction capacity of 35 W), the first deployment gave an average efficiency of 0.403% while the second deployment gave an average efficiency of 4.143%. When compared with the efficiencies of similar devices that are currently operational (Wavebob – efficiency 40-51%, AquaBuoy – efficiency 17-21%, and Sea Dog – efficiency 16-24%), this technology still needs certain modifications and optimisations to improve performance efficiency-wise. However, when compared to solar PV efficiency (15-20% typically), this technology can be highly beneficial if the availability factor (four times of solar energy availability) is also taken into consideration. Based on observations made on the device performance and behaviour during the deployments, the irregularities in the incident waves, sand particle interaction with certain components of the submerged system, and mechanical losses, lead to losses in device performance. Out of these, mechanical losses in the transmission system and drive system such as rubbing of the chains against chain guides and the sliding friction between the components of the energy extraction system were found to be the major contributors for energy losses. Furthermore, it was evident that the dimensions of the device should be further fine-tuned to match the topography of the sea environment where the device is planned to install in. This way, the device can be made more responsive to the incoming waves for energy extraction. Once these issues are addressed, the device can be made more efficient in extracting wave energy.

5. Conclusion

This paper presented a novel WEC that is aimed to reduce both capital and operational expenditure while maximising device performance. Accordingly, the WEC was designed to be able to capture both the kinetic and potential energy formats of the sea waves regardless of the wave propagation direction.

- Designed device is capable of delivering 1.45 W of power on average with an efficiency of 4.143% when operated at the test site.

- Out of the two flap types considered, computational fluid dynamic (CFD) simulations revealed that the prismatic shell type flap arrangement is superior to the cylindrical shell type flap arrangement in terms of hydrodynamic performance.

- Considering ease of fabrication also, prismatic shell type flap is preferred over the cylindrical shell type flap.

- Hydrodynamic simulations revealed that the device can be used to extract both kinetic energy and potential energy from sea waves. This makes the device more effective in energy extraction.

- Hydrodynamic simulation results can be used for optimisation of the device by adjusting inertial and geometric parameters of the proposed device.

- When comparing the recorded highest efficiency of 4.143% with currently available technologies that use similar techniques, further development and optimisation would be necessary to make this technology more economically viable.

- Mechanical losses, wave irregularities, slow device response to incident waves, and sand particle interaction with the device are observed to be major contributors for the limited device performance.

- Since the power conversion system is designed to be stationed away from the sea, maintenance of the device can be made easier and cheaper.

Hence, above insights can be used in designing scaled-up WEC devices with better effectiveness and economic viability. Future works on this study would include comprehensive fluid dynamic modelling, analysis, and optimisation of different designs to improve hydrodynamic performance of the WEC and more field tests involving real time data logging. Also, more focus to be given for selecting reliable materials for different components of the WEC to minimise corrosion and frictional losses, while reducing the overall weight. Furthermore, the effect of wave break should also be studied in order to determine most suitable installation locations. Such research and development works will ensure reliable and efficient operation of the WEC to generate green power from sea waves.

Acknowledgement

Authors wish to acknowledge the Undergraduate Research Project funding available at the Faculty of Engineering, University of Ruhuna, Sri Lanka and also the workshop facilities of the Department of Mechanical and Manufacturing Engineering of the same Faculty. Also, the authors acknowledge the assistance received from Eng. H.P.O.N. Yasarathna for fabrication works and experimental testing of the physical model.

References

1. Lelieveld, J., Klingmüller, K., Pozzer,A., Burnett, R. T., Haines, A., and Ramanathan, A.,"Effects of Fossil Fuel and Total Anthropogenic Emission Removal on Public Health and Climate," *Proc. Natl. Acad. Sci. U. S. A.*, Vol. 116, No. 15, pp. 7192–7197, 2019, doi: 10.1073/pnas.1819989116.

2. Muzathik, A. M., Nik, W. M. N. B. W., Bin Samo, K., Ibrahim, M. Z., and Said, M. H., "Ocean Wave Energy Potential and Extraction Technologies," in *Proceedings of the 6th Marine Technology Conference, Indonesia*, 2008, No. August.

3. Sun, C., Shang, J., Luo, Z.,Lu, Z., and Wang, R., "A Review of Wave Energy Extraction Technology," *IOP Conf. Ser. Mater. Sci. Eng.*, Vol. 394, No. 4, 2018, doi: 10.1088/1757-899X/394/4/042038.

4. Amarasekara *et al.*, H. W. K. M., "A Prefeasibility Study On Ocean Wave Power Generation For The Southern Coast of Sri Lanka: Electrical Feasibility," *Int. J. Distrib. Energy Resour. Smart Grids*, Vol. 10, No. 2, pp. 79--93, 2014.

5. Lokuliyana,R.L.K., Folley, M., Gunawardane, S.D.G.S.P., and Wickramanayake, P.N., "Sri Lankan Wave Energy Resource Assessment and Characterisation Based on IEC Standards," *Renew. Energy*, vol. 162, pp. 1255–1272, 2020, doi: 10.1016/j.renene. 2020.08.005.

6. Clément *et al.*, A., "Wave Energy in Europe: Current Status and Perspectives," *Renew. Sustain. Energy Rev.*, Vol. 6, No. 5, pp. 405–431, 2002, doi: 10.1016/S1364-0321(02)00009-6.

7. Rusu, E., and Onea, F., "Review Article A Review of the Technologies for Wave Energy Extraction," *Clean Energy*, No. April, pp. 1–10, 2018, doi: 10.1093/ce/zky003.

8. Drew, B., Plummer, A. R., and Sahinkaya, M. N., "A Review of Wave Energy Converter Technology," *Proc. Inst. Mech. Eng. Part A J. Power Energy*, Vol. 223, No. 8, pp. 887–902, 2009, doi: 10.1243/09576509JPE782.

9. Aderinto, T., and Li, H., "Review on Power Performance and Efficiency of Wave Energy Converters," *Energies*, Vol. 12, No. 22, pp. 1–24, 2019, doi: 10.3390/en12224329.

10. Astariz, S., and Iglesias, G., "Enhancing Wave Energy Competitiveness through Co-Located Wind and Wave Energy Farms. A Review on the Shadow Effect," *Energies*, Vol. 8, No. 7, pp. 7344–7366, 2015, doi: 10.3390/en8077344.

11. "Why Does the Ocean have Waves?" https://oceanservice.noaa.gov/facts/wavesinocean.html (accessed Sep. 23, 2020).

12. Giorgi, G., and Ringwood, J. V., "Analytical Representation of Nonlinear Froude-Krylov Forces for 3-DoF Point Absorbing Wave Energy Devices," *Ocean Eng.*, Vol. 164, No. December 2017, pp. 749–759, 2018, doi: 10.1016/j.oceaneng.2018.07.020.

13. Babarit, A., Mouslim, H., Cle´ment, A., and Laporte-Weywada, P., "On the Numerical Modelling of the Non Linear Behaviour of a Wave Energy Converter," in *Proceedings of the ASME 2009 28th International Conference on Ocean, Offshore and Arctic Engineering*, 2009, Vol. Volume 4:, pp. 1045–1053, doi: 10.1115/OMAE2009-79909.

14. Evans, D. V., Jeffrey, D. C., Salter, S. H., and Taylor, J. R. M., "Submerged Cylinder Wave Energy Device: Theory and Experiment," *Appl. Ocean Res.*, Vol. 1, No. 1, pp. 3–12, 1979, doi: 10.1016/0141-1187(79)90003-8.

15. E.-S. Aziz, Chassapis, C., Dai, S., and Xu, S., "Online Wind Tunnel Laboratory," in *ASEE Annual Conference and Exposition*, 2008, No. March 2015, doi: http://dx.doi.org/10.18260/1-2--3402.